Positron Transmission Imaging of Histological Slices

Adrien Hourlier V. Bekaert, F. Boisson, D. Brasse
IPHC
04/10/2023

adrien.hourlier@iphc.cnrs.fr

Changing PET paradigm

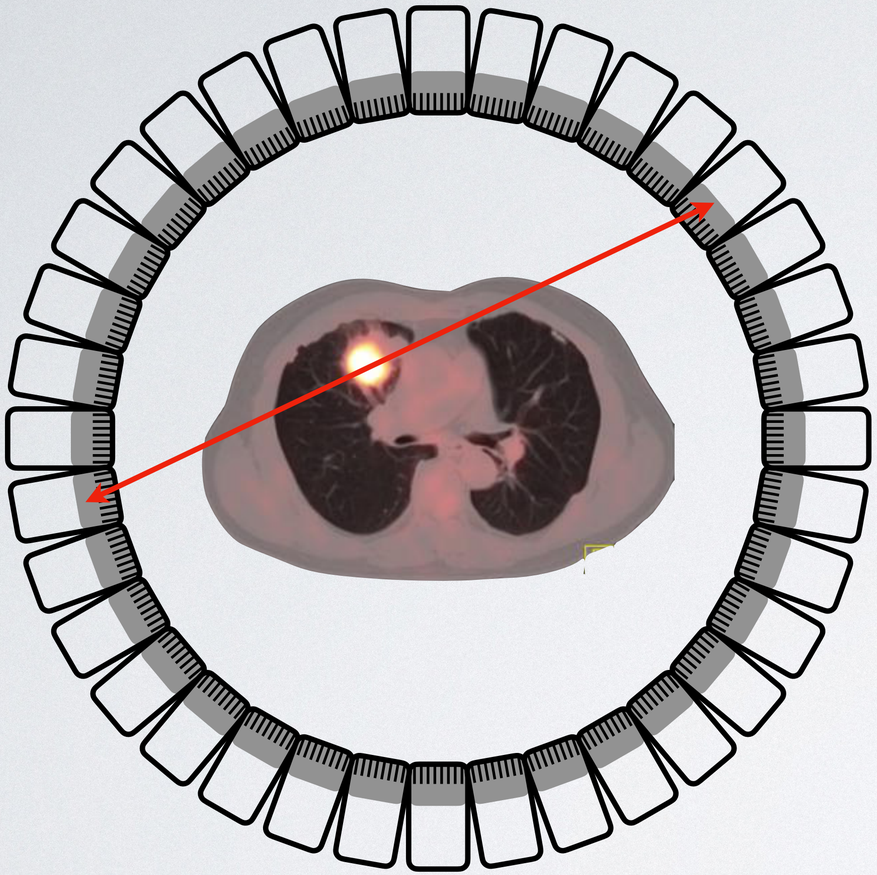

- PET relies on 2γ pair coincidences from e^+e^- annihilation to reconstruct the spatial distribution of a radiotracer
- Multiple separate frames : temporal evolution of the spatial distribution :
  - compartmental analysis
  - pharmacokinetics,
  - …
- Tissues that exhibit the desired biological function get highlighted, but no other information on that tissue
  - **More information** is encoded in the annihilation itself
  - How can we access it ?

Positronium annihilation

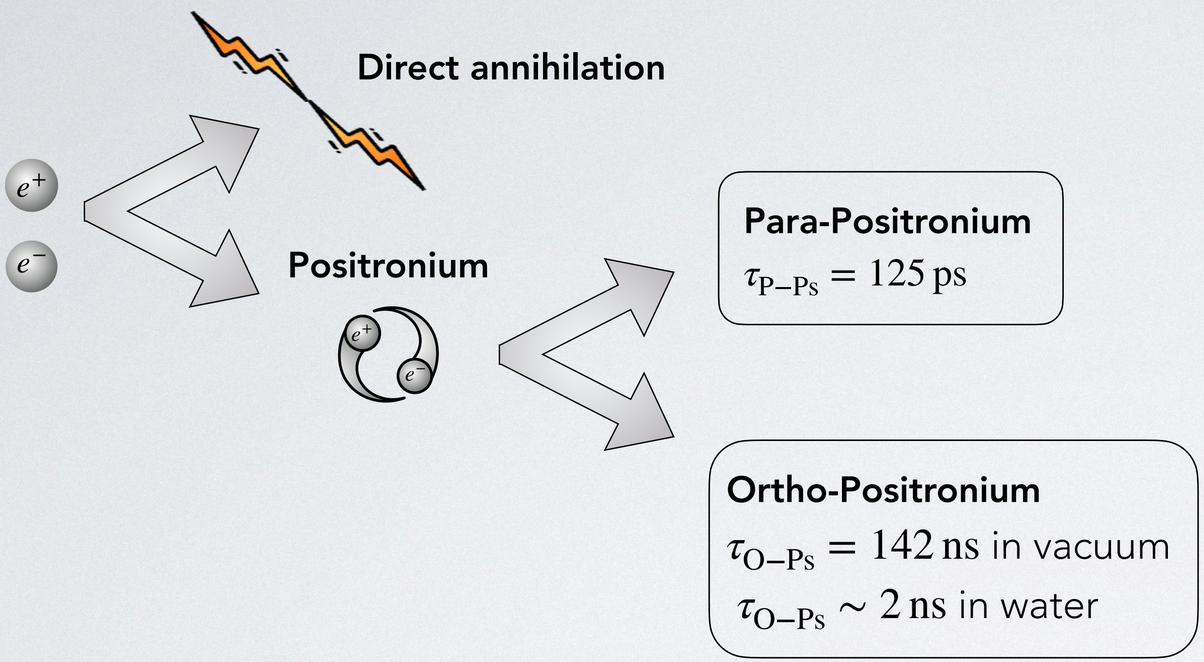

Para-Positronium

$\tau_{P-Ps} = 125\,ps$

Ortho-Positronium

$\tau_{O-Ps} = 142\,ns$ in vacuum

$\tau_{O-Ps} \sim 2\,ns$ in water

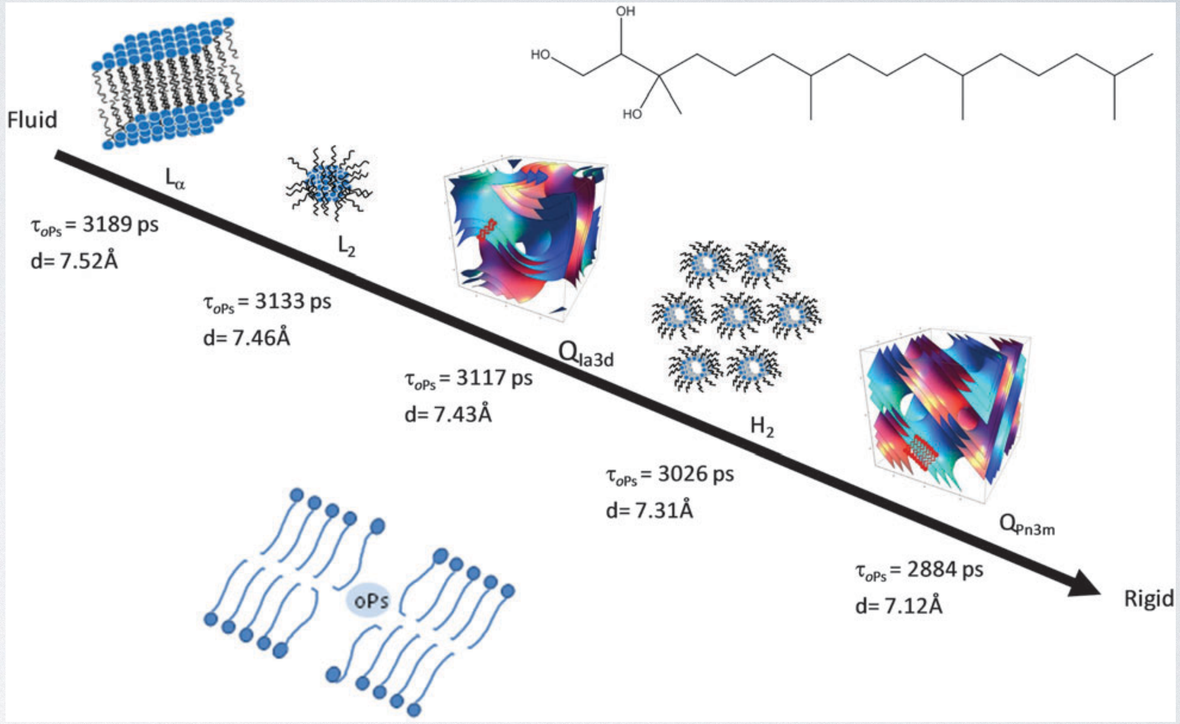

C Fong et al. Phys. Chem. Chem. Phys., 2015,17, 17527-17540

Ortho-postironium formation probability and lifetime depends on the medium

- size of free volume (atomic to molecular level vacuum)
- presence of electronegative regions

Widely used in material science to study microstructures, defects, porosity

⇒Can we use it in PET?

Some studies on biological samples

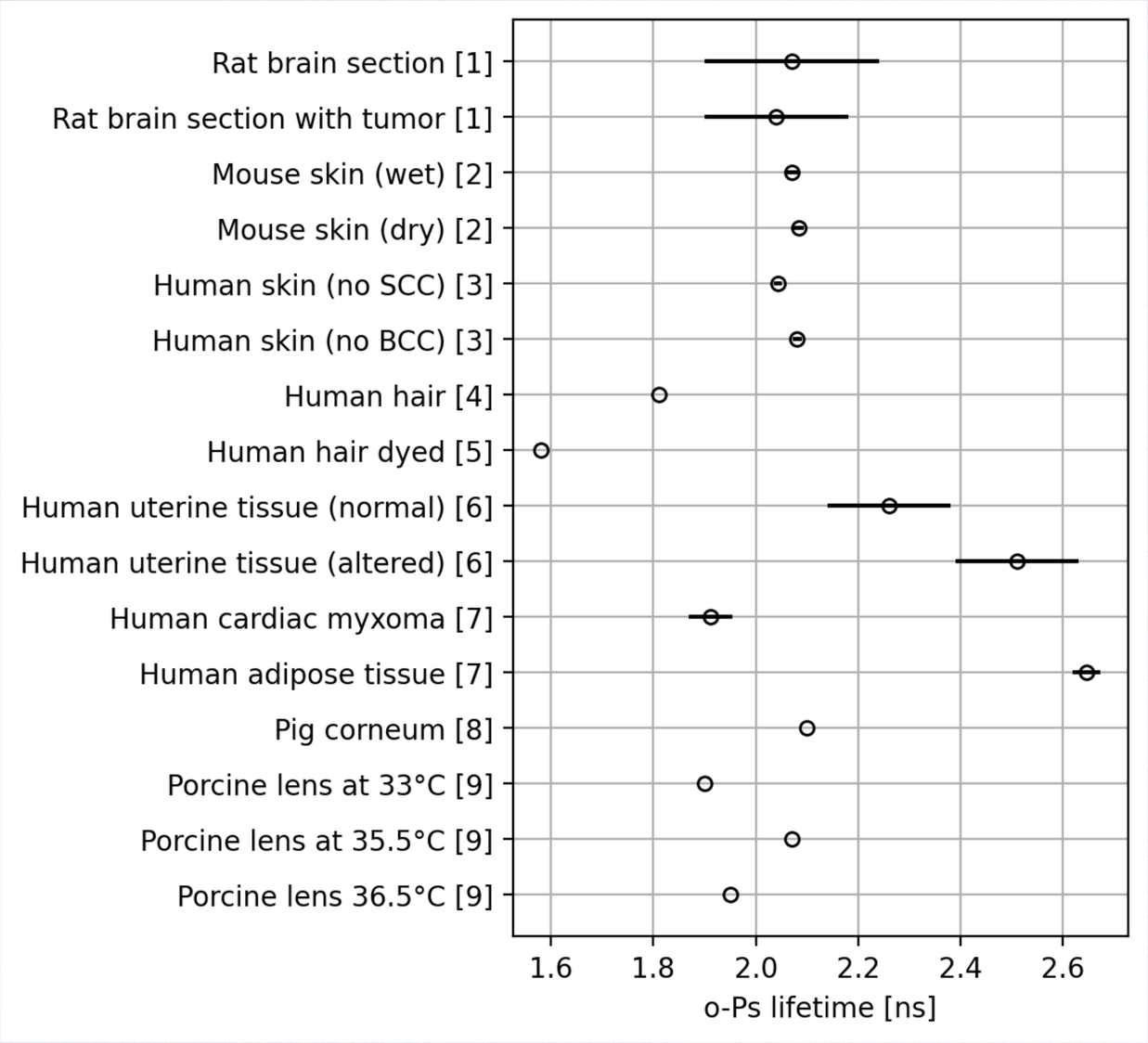

- Mostly around 2 ns : need excellent resolution power.
- Patient-patient variability often larger than between tissues of a same patient
- Experimental protocole variations between these studies could yield non-negligible variability.
- Tissue sample size : averaging of measured lifetime for many types of tissues lowers the separation power.

(1) SH Yang, et al. 2009. https://doi.org/10.1063/1.3120199
(2) Jean, Y. C., et al. 2007. https://doi.org/10.1016/j.radphyschem.2006.03.008
(3) Jean, Y. C., et al. 2006. https://doi.org/10.1016/j.apsusc.2005.08.101
(4) Chandrashekara, M. N., et al. 2010. https://doi.org/10.1016/j.jphotobiol.2010.07.014
(5) Chandrashekara, M. N., et al. 2009. https://doi.org/10.1016/j.colsurfb.2008.11.014
(6) Jasińska, B., et al. 2017. http://dx.doi.org/10.12693/APhysPolA.132.1556
(7) Moskal, Paweł, et al. 2021. https://doi.org/10.1126/sciadv.abh4394
(8) Itoh, Yoshiaki, et al. 2008. https://doi.org/10.1016/j.ijpharm.2008.02.016
(9) Sane, Petri, et al. 2010. https://doi.org/10.1016/j.bbamem.2010.01.011

Changing PET paradigm

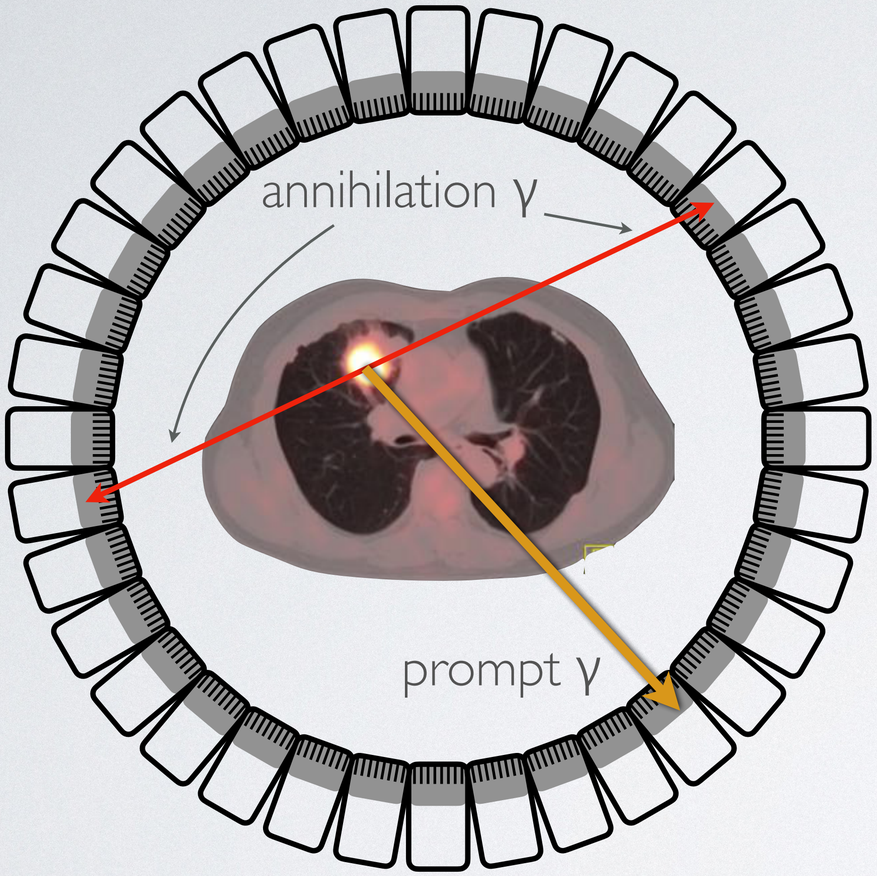

Measuring $\tau_{\mathrm{O-Ps}}$:

- Challenge : 3D, in vivo Positron annihilation lifetime spectroscopy (PALS)
- Need to access the O-Ps annihilation time
  - Prompt γ emitted as part of a (β^+,γ) decay
  - 3γ coincidence
    - High efficiency PET
    - High coverage PET : full body scanner?
    - Xemis-2, J-PET, uExplorer
    - What isotope? with realistic existing radio-chemistry?
  - High coincidence time resolution
    - able to separate small $\tau_{\mathrm{O-Ps}}$ differences

Proof of concept : J-PET Ex-vivo

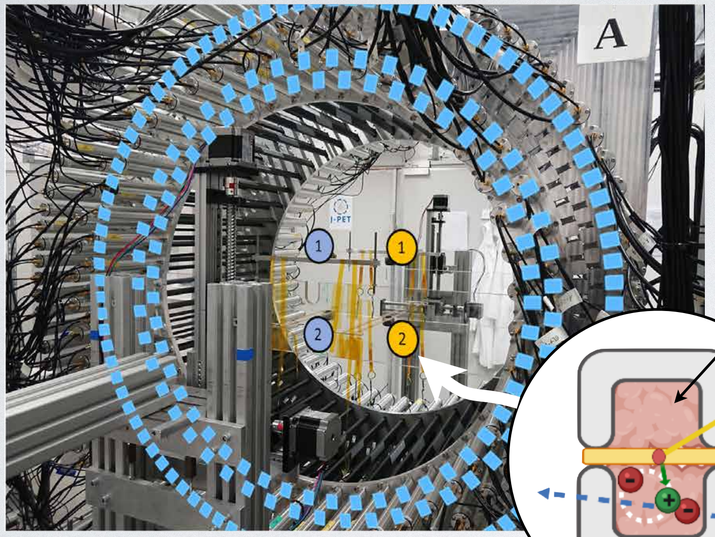

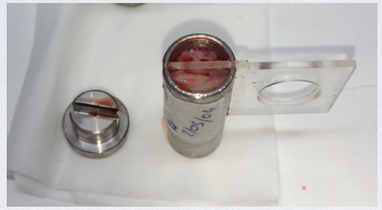

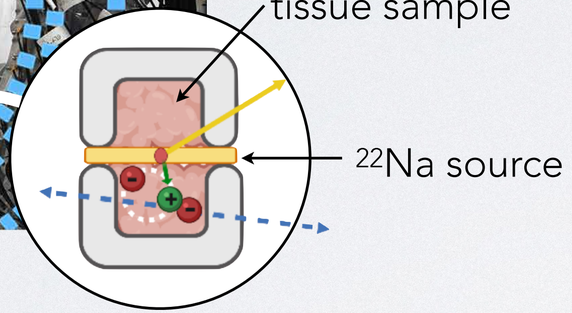

- Demonstration of J-PET's ability to measure τ_{O-Ps}
- Four separate samples in the field of view
- Direct contact to a ^{22}Na (β^+,γ)source

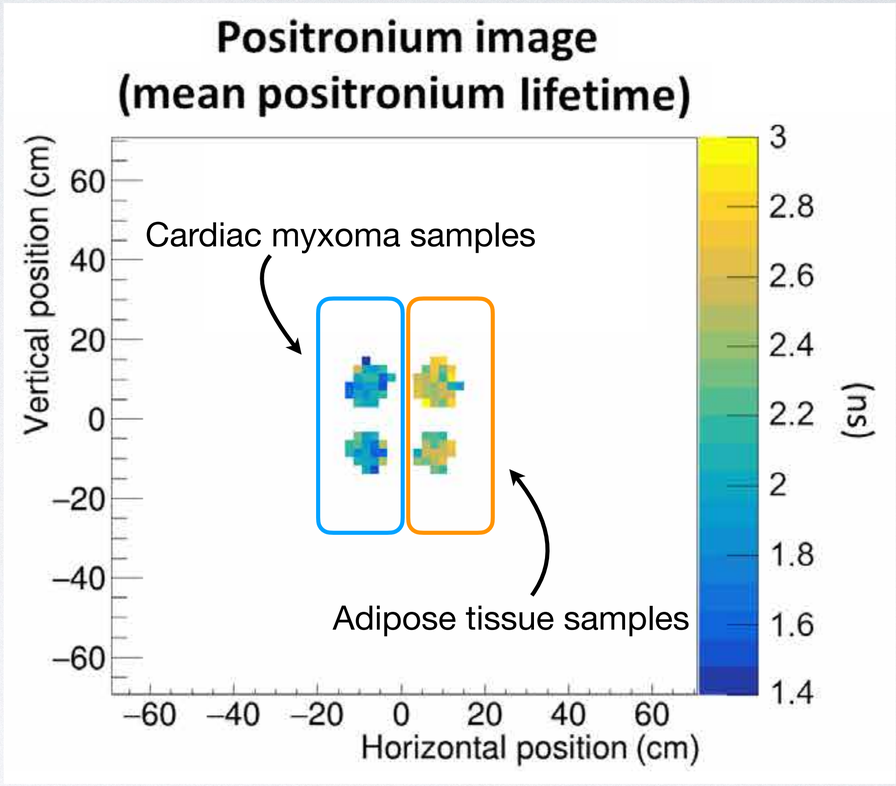

Moskal, Paweł, et al. 2021. https://doi.org/10.1126/sciadv.abh4394

Proof of concept : J-PET

In-vivo

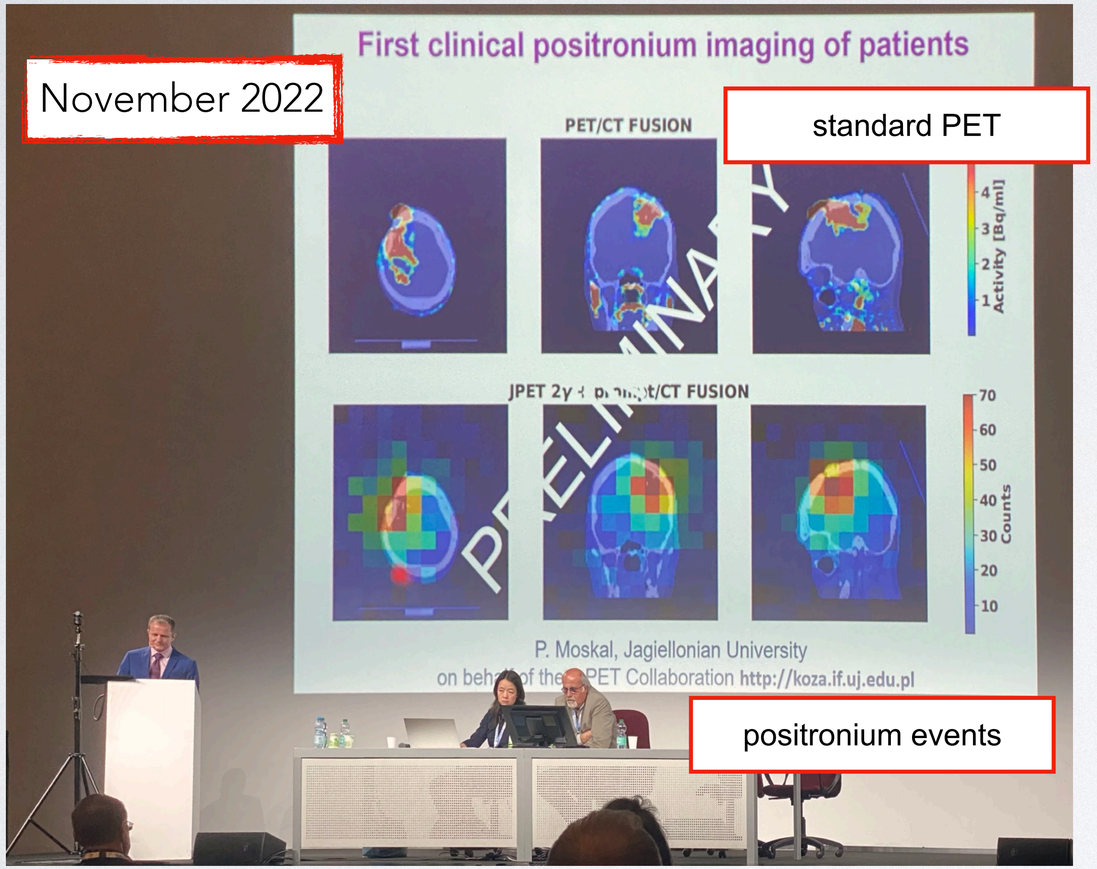

Limitations :

- need to be able to fit the lifetime distribution:
  need high statistics in each voxel
  ⇒ need large voxels or high activity
- measurement only possible where the tracer is located :
  what additional information from the biodistribution?
  how various tissues will affect the measured lifetime?

Imager des tissus par τ_{O-Ps}

coupe histologique
cerveau de souris

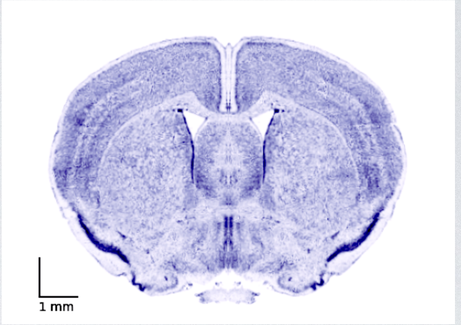

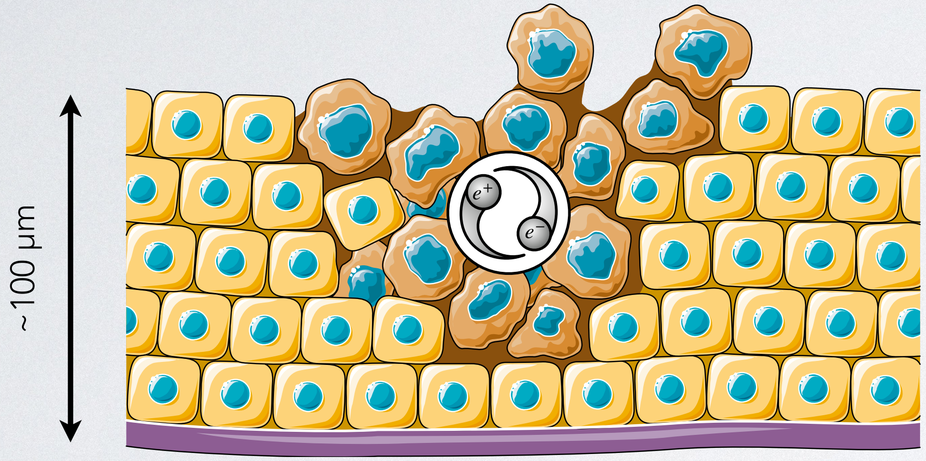

- **TRI**ple **C**oincidence **E**vents from β⁺ **RA**dioisotopes to image **τ_{O-Ps}**

Imager des tissus par τ_{O-Ps}

coupe histologique
cerveau de souris

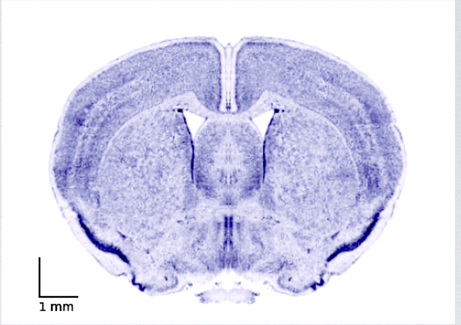

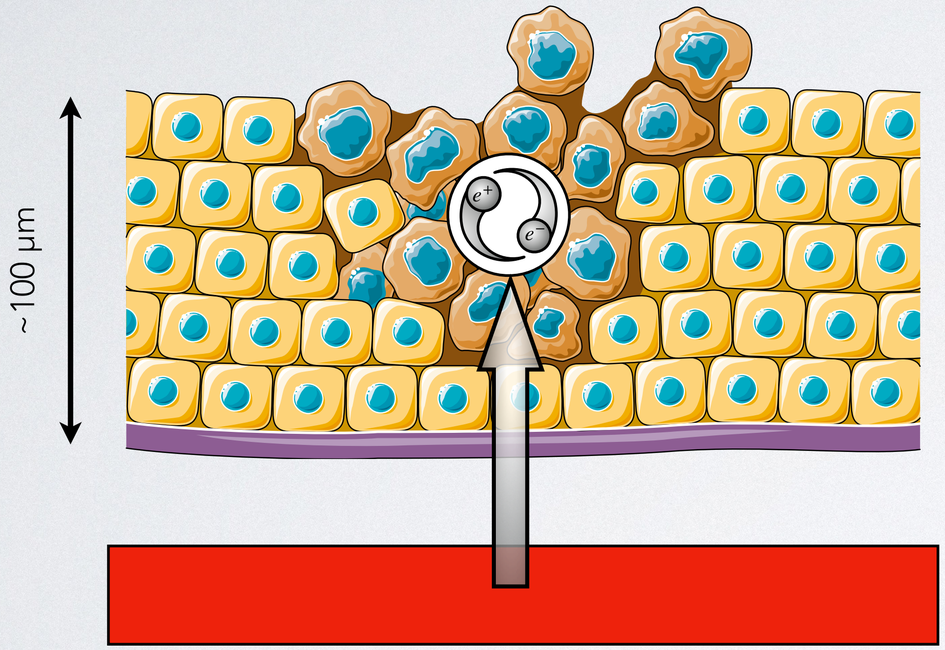

- **TRI**ple **C**oincidence **E**vents from β⁺ **RA**dioisotopes to image **τ_{O-Ps}**
- Mesurement **indépendant from radiotracer biodistribution**

Imager des tissus par τ_{O-Ps}

coupe histologique
cerveau de souris

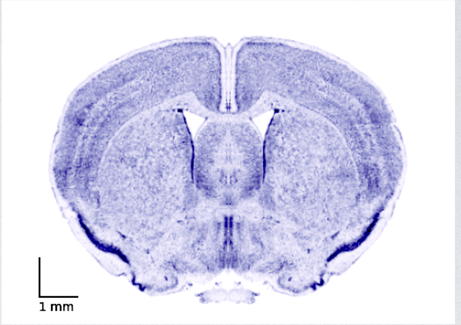

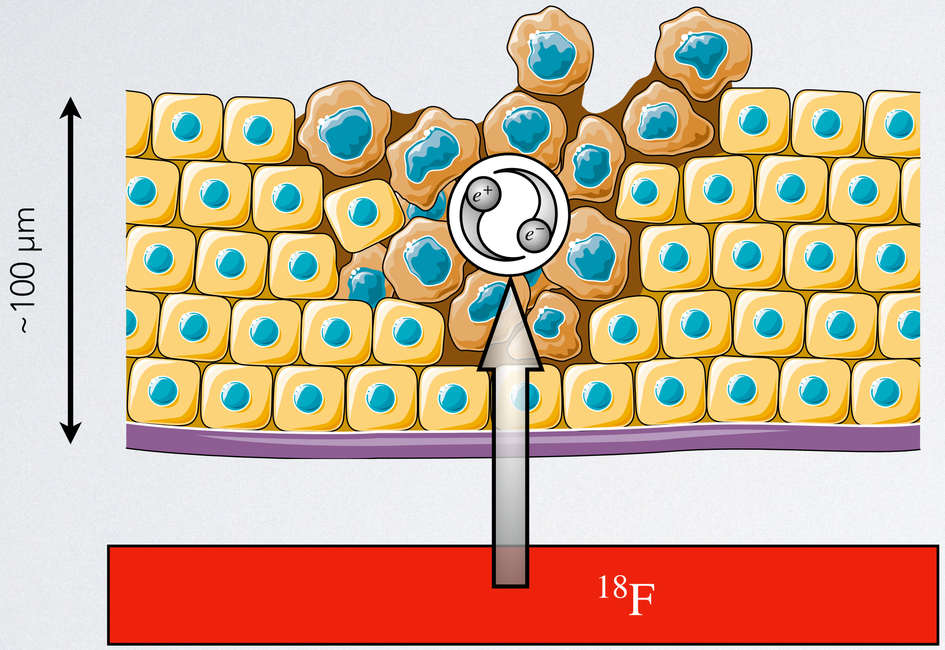

- **TRI**ple **C**oincidence **E**vents from β⁺ **RA**dioisotopes to image **TO-Ps**
- Mesurement **indépendant from radiotracer biodistribution**

Imager des tissus par τ_{O-Ps}

coupe histologique
cerveau de souris

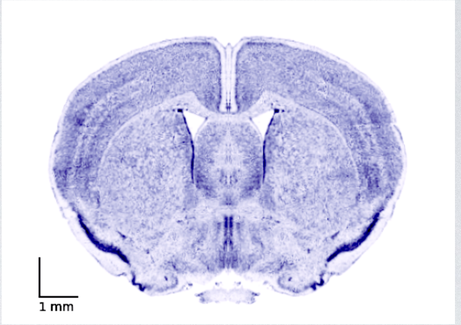

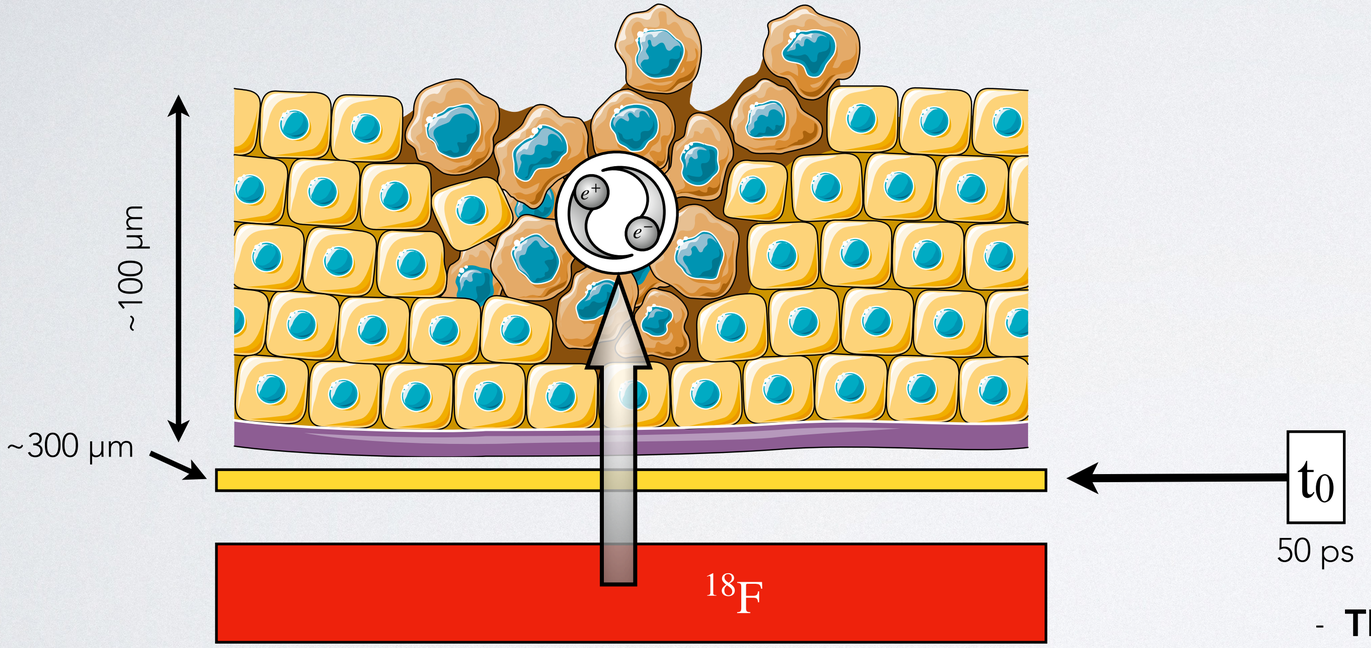

t_0
50 ps

- **TRI**ple **C**oincidence **E**vents from β⁺ **RA**dioisotopes to image **τ_{O-Ps}**
- Mesurement **indépendant from radiotracer biodistribution**

Imager des tissus par τ_{O-Ps}

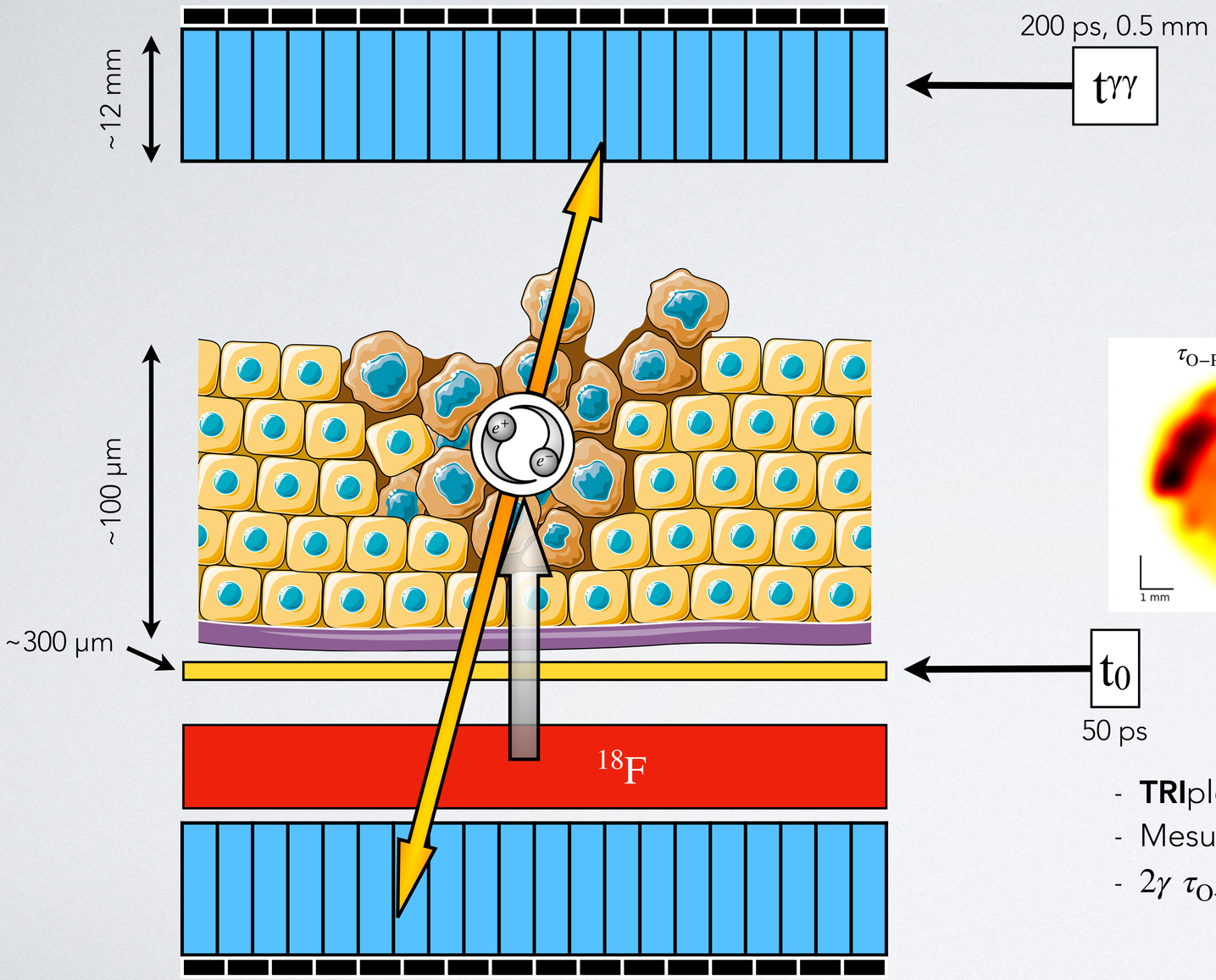

coupe histologique
cerveau de souris

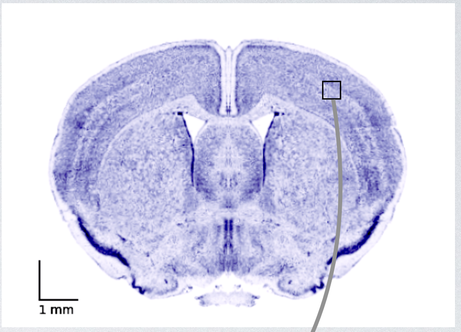

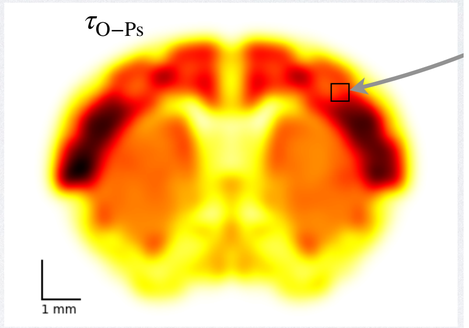

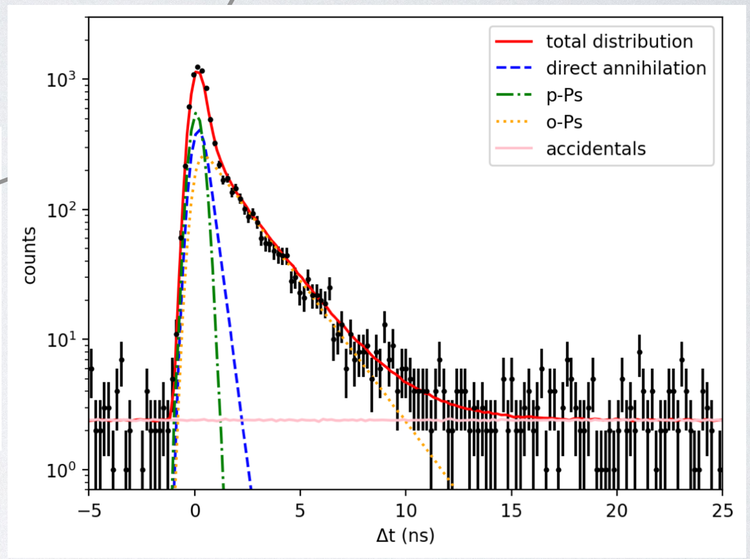

- **TRI**ple **C**oincidence **E**vents from β⁺ **RA**dioisotopes to image **T_{O-Ps}**
- Mesurement **indépendant from radiotracer biodistribution**
- 2γ τ_{O-Ps} **Imaging** : usual β⁺ isotopes (^{18}F)

Imager des tissus par τ_{O-Ps}

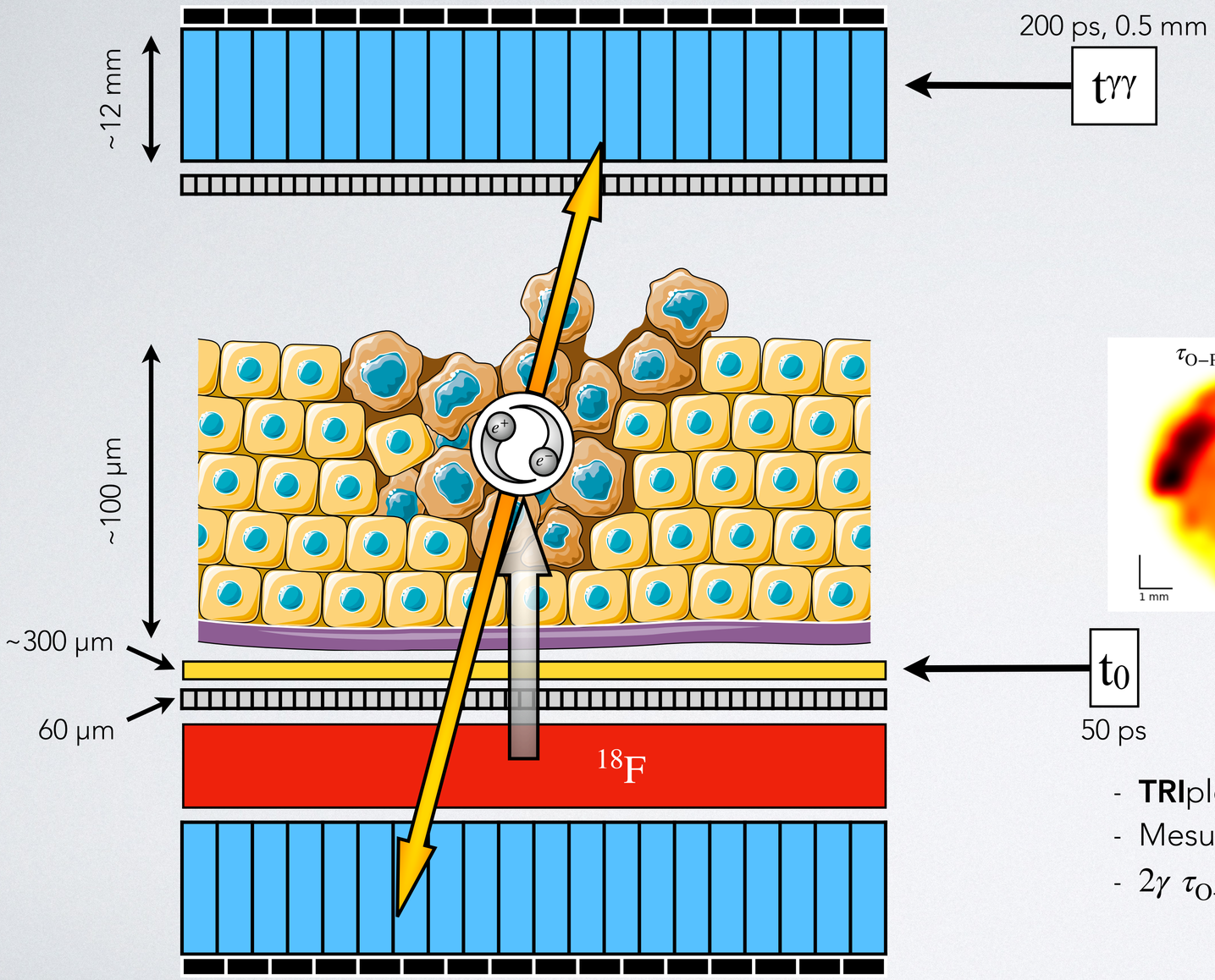

coupe histologique
cerveau de souris

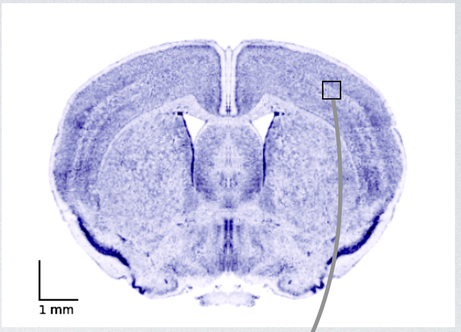

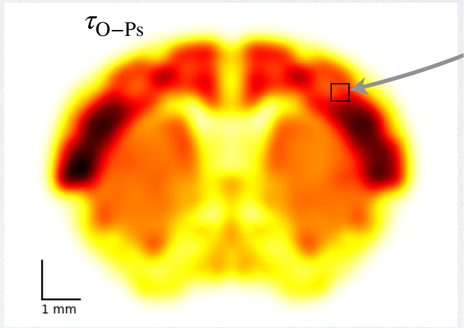

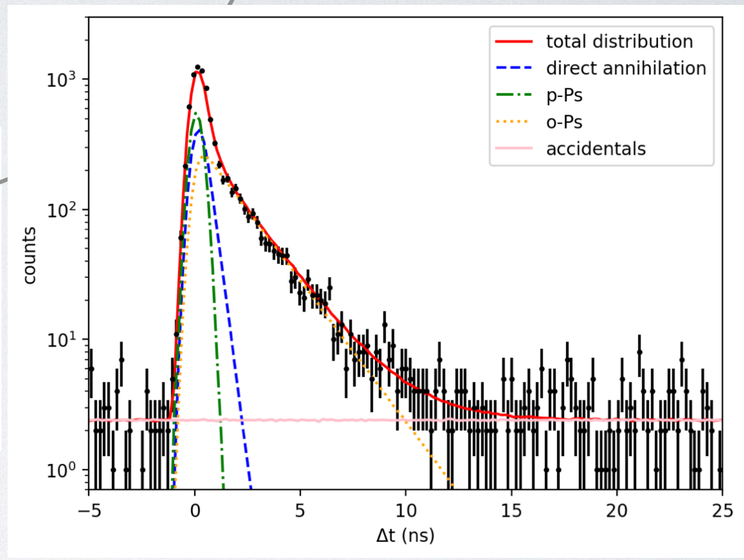

- **TRI**ple **C**oincidence **E**vents from β⁺ **RA**dioisotopes to image **T_{O-Ps}**
- Mesurement **indépendant from radiotracer biodistribution**
- 2γ τ_{O-Ps} **Imaging** : usual β⁺ isotopes (^{18}F)

Imager des tissus par τ_{O-Ps}

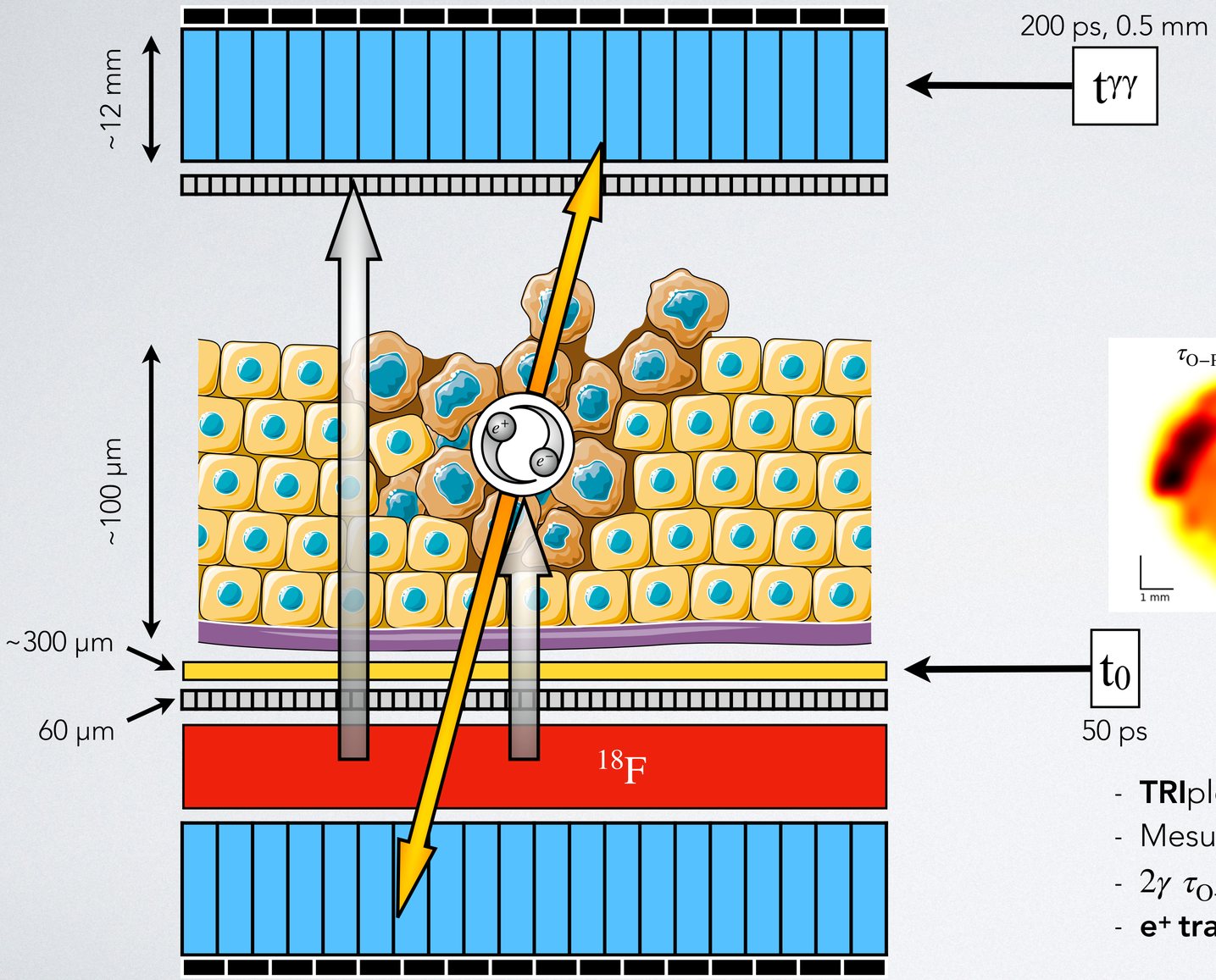

coupe histologique
cerveau de souris

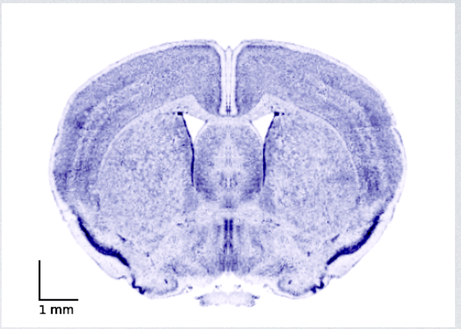

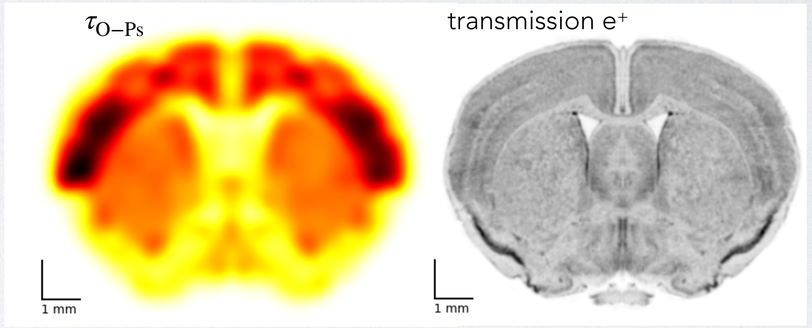

- **TRI**ple **C**oincidence **E**vents from β⁺ **RA**dioisotopes to image **T_{O-Ps}**
- Mesurement **indépendant from radiotracer biodistribution**
- 2γ τ_{O-Ps} **Imaging** : usual β⁺ isotopes (^{18}F)
- **e^+ transmission** imaging

Imager des tissus par τ_{O-Ps}

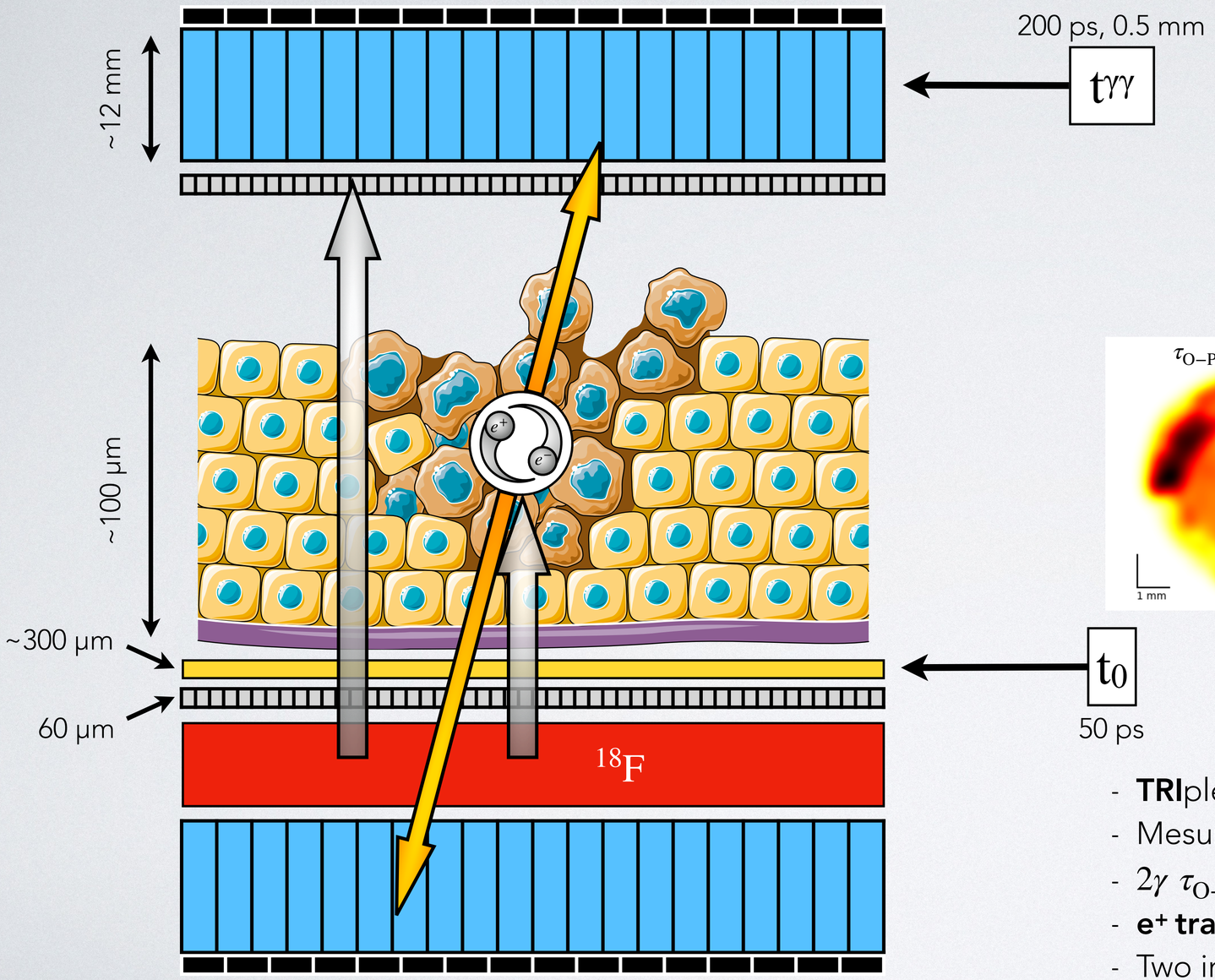

coupe histologique
cerveau de souris

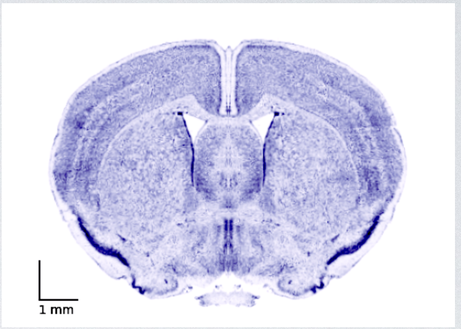

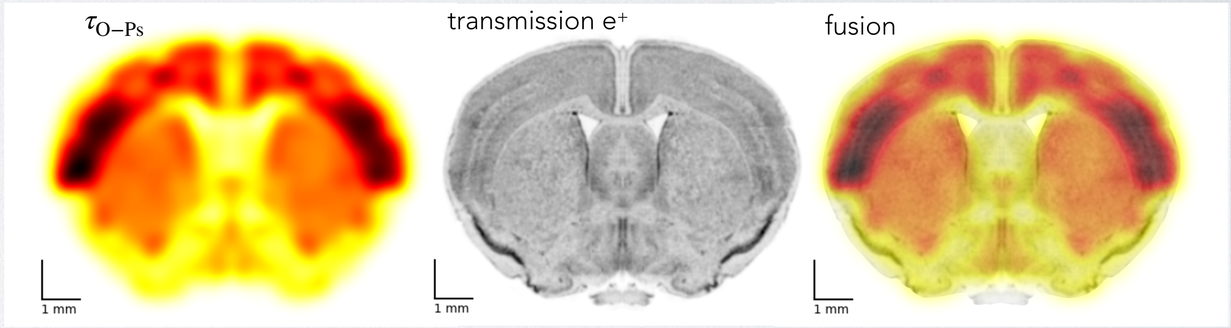

- **TRI**ple **C**oincidence **E**vents from β⁺ **RA**dioisotopes to image **T_{O-Ps}**
- Mesurement **indépendant from radiotracer biodistribution**
- 2γ τ_{O-Ps} **Imaging** : usual β⁺ isotopes (^{18}F)
- **e^+ transmission** imaging
- Two imaging modalities acquired **simultaneously**

Various pixellated layer technology choices

CMOS sensor

- e.g. MIMOSIS-1, developed @IPHC
- 30x27 μm^2 pixels
- 60µm total thickness
- 5µs readout time
- Large readout surface 31.1x13.55 mm^2

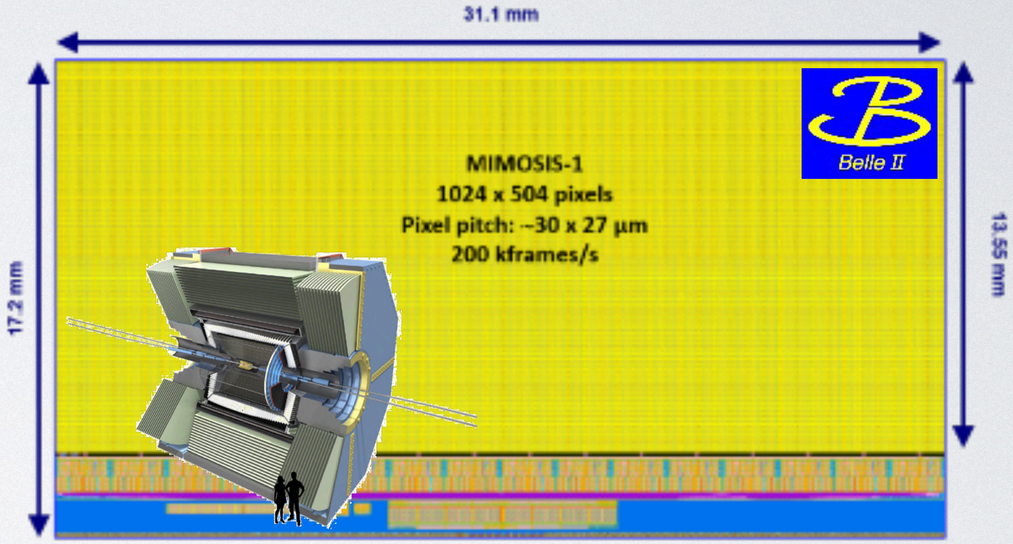

Other possibilities

- MicroMegas
- (X,Y) oriented MWPC
- optical fiber-based hodoscope

Simulated geometry & event selection

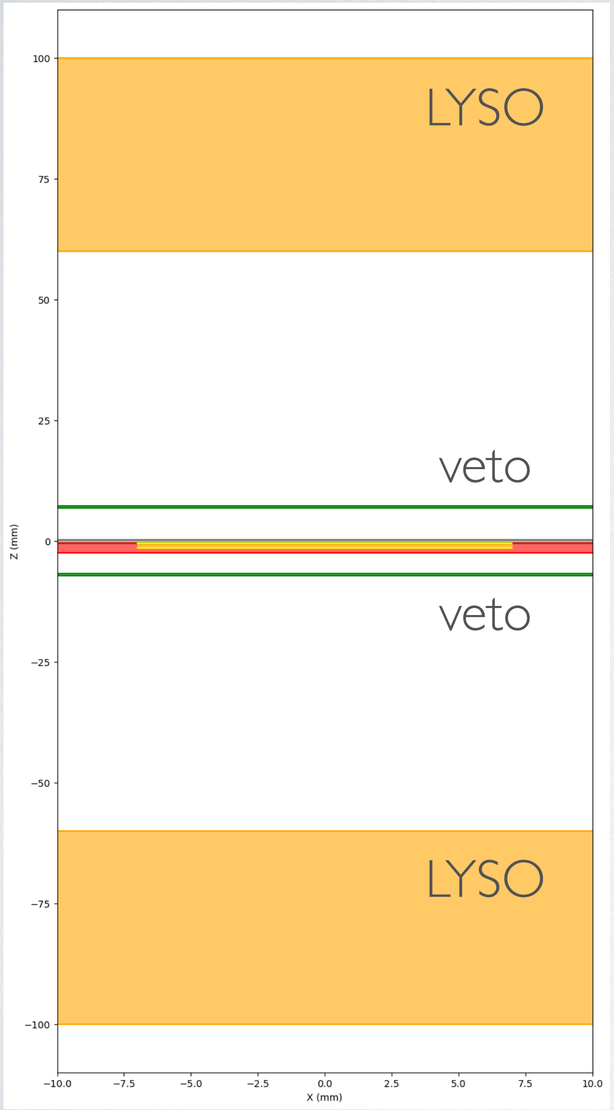

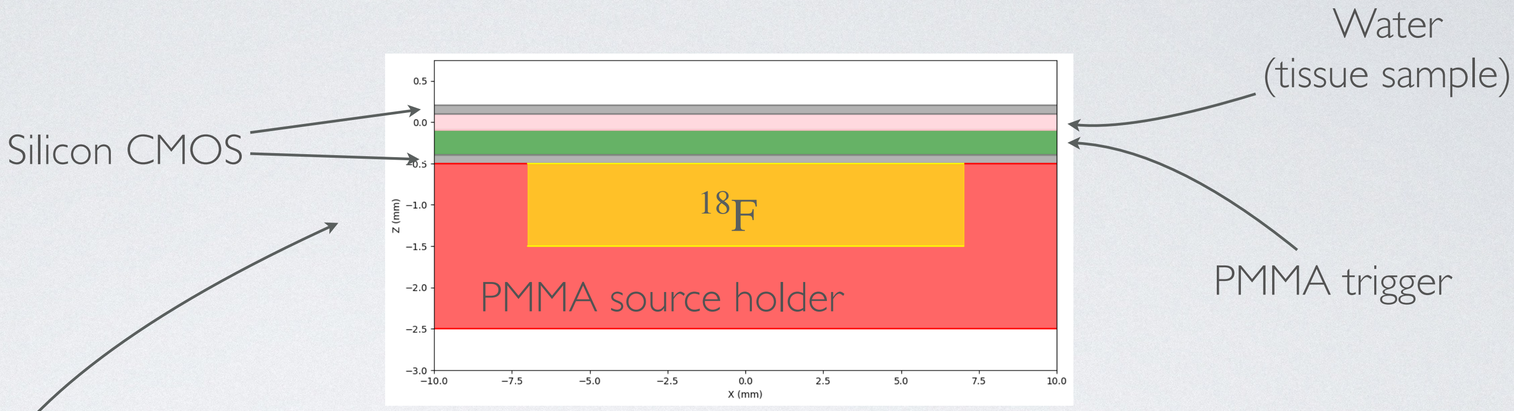

- PET detectors : 4 cm-thick LYSO blocks, 500 µm pixel pitch
- Pixellated layer : Silicon, 100 µm-thick, 50 µm pixel pitch
- Trigger and vetoes : PMMA (respectively 300 µm and 500 µm)
- Tissue : water 200 µm-thick + Si insert (phantom)

PET selected event :

- trigger ⊕ upstream pixel ⊕ NO downstream pixel ⊕ NO veto ⊕ top PET ⊕ bottom PET
- 0.019% of decays (190 cps/MBq)

Transmission event :

- trigger ⊕ upstream pixel ⊕ downstream pixel ⊕ NO veto
- 0.092 % of decays (920 cps/MBq)

Transmission Image Reconstruction

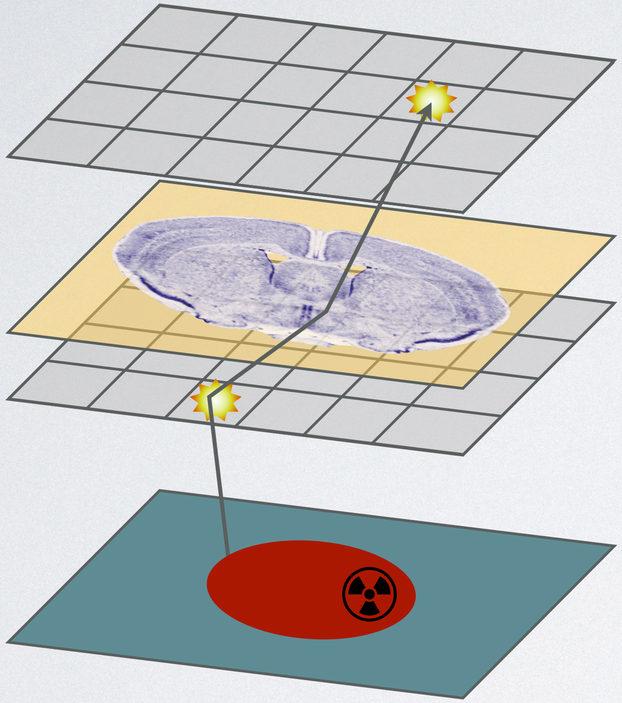

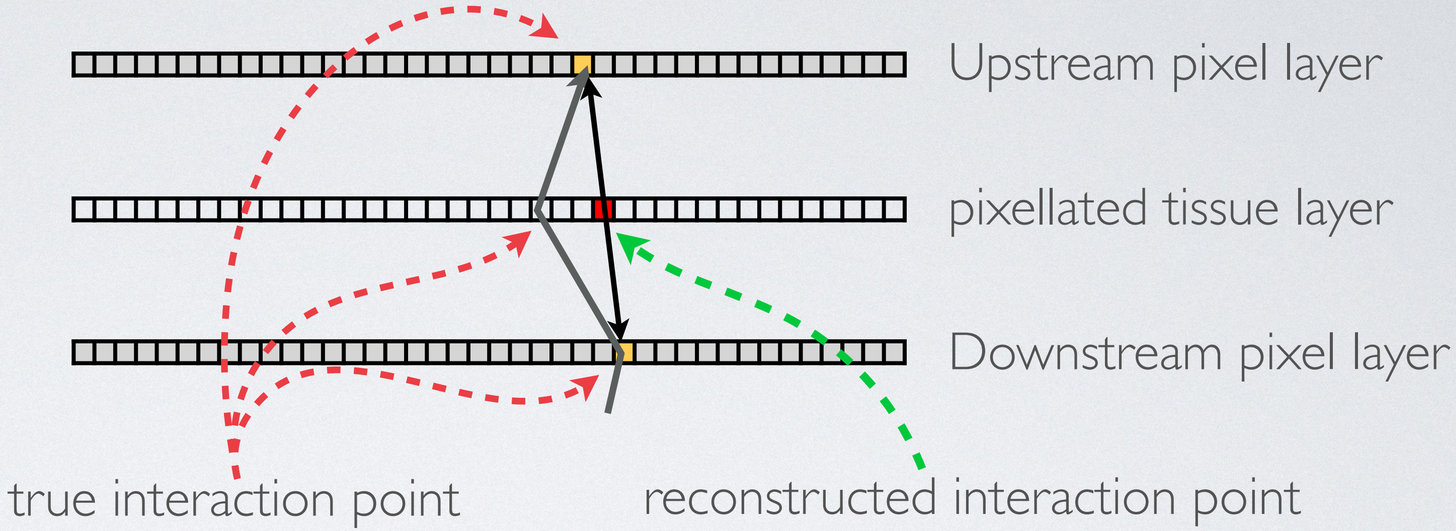

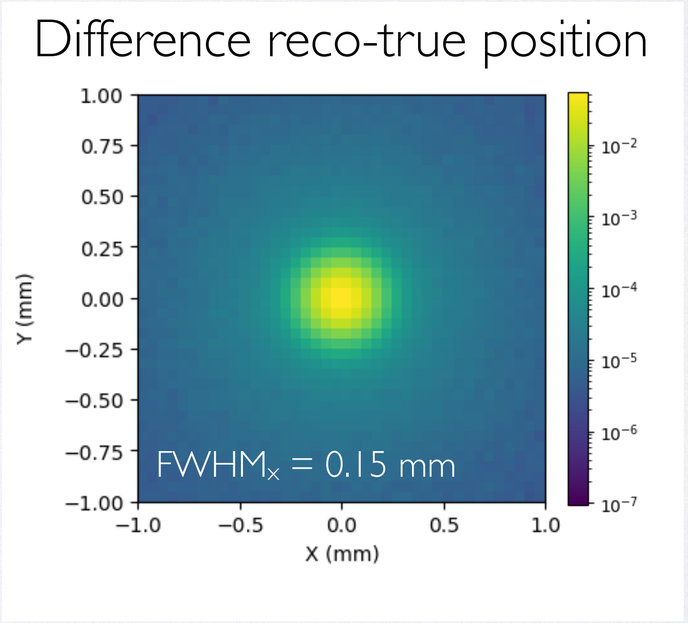

Transmission Image Reconstruction

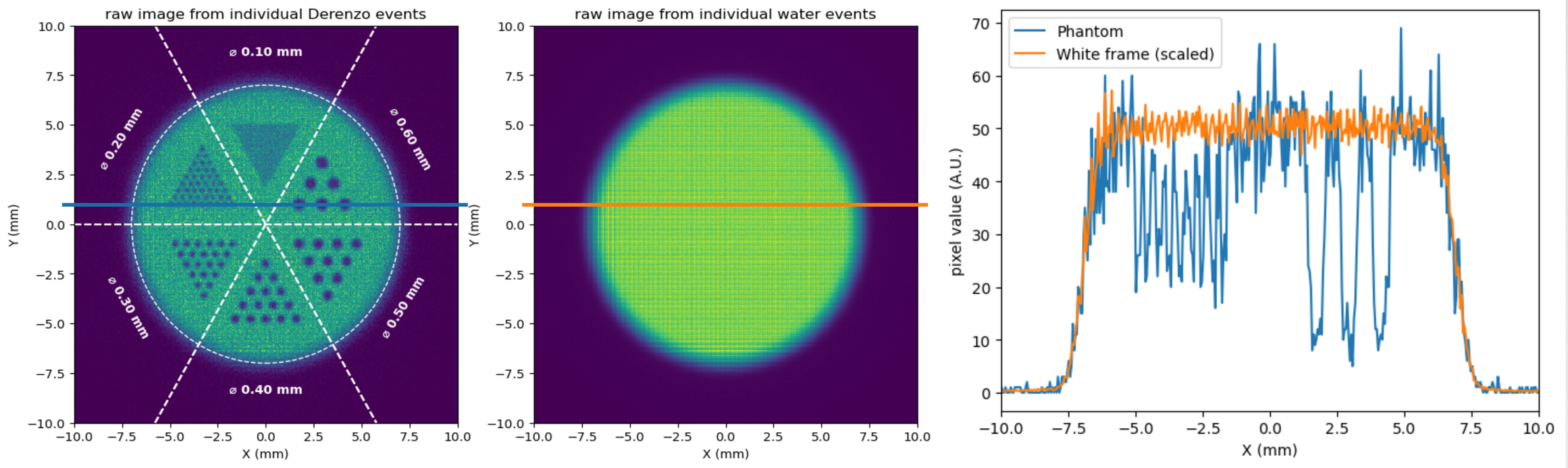

Derenzo phantom
10 min @ 5MBq

"White" frame (water)
9h @ 5MBq

Attenuation coefficient

- Assume that the attenuation of positron beam follows the Beer Lamber law :
- $I(x,y) = I_0(x,y) \cdot e^{-\mu(x,y)\cdot\langle\Delta z\rangle}$
- $I_0(x,y)$ is given by the pure water white frame
- $\langle\Delta z\rangle$ is the average thickness travelled in the layer by the positron
- Attenuation coefficient image :

$$\mu(x,y) = -\frac{1}{\langle\Delta z\rangle}\ln\left(\frac{I(x,y)}{I_0(x,y)}\right)$$

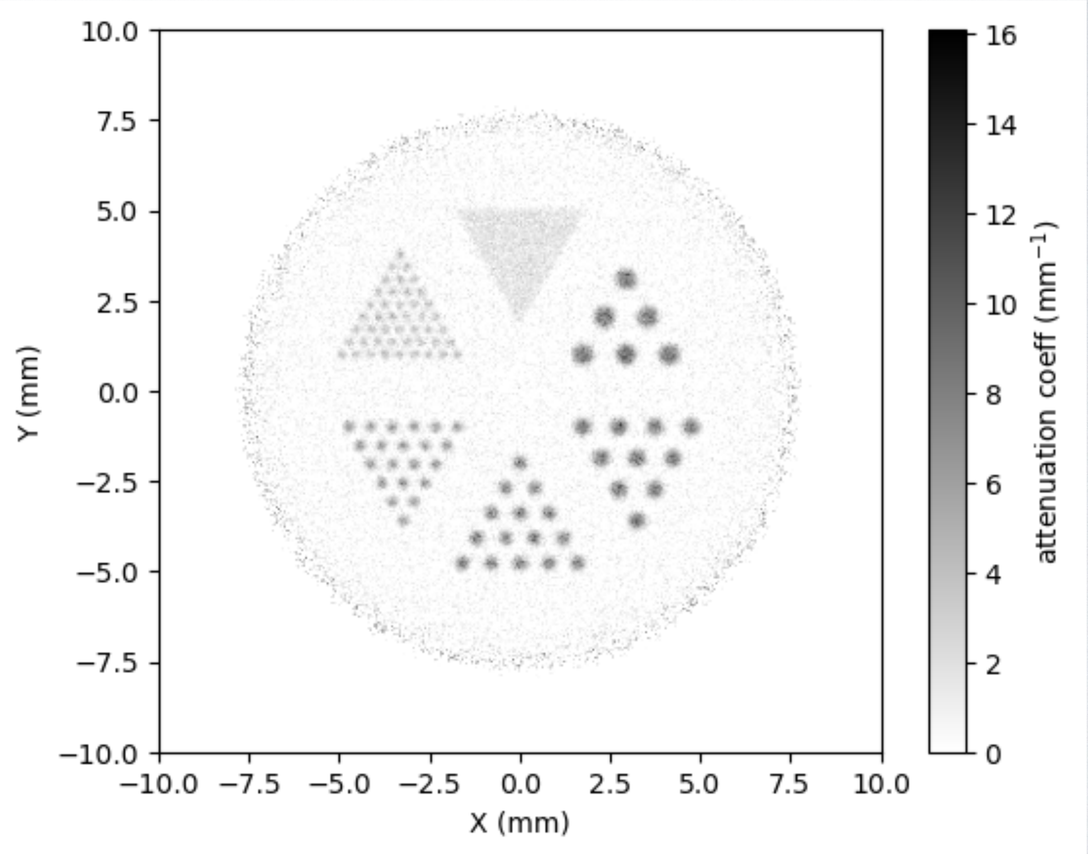

Profiles

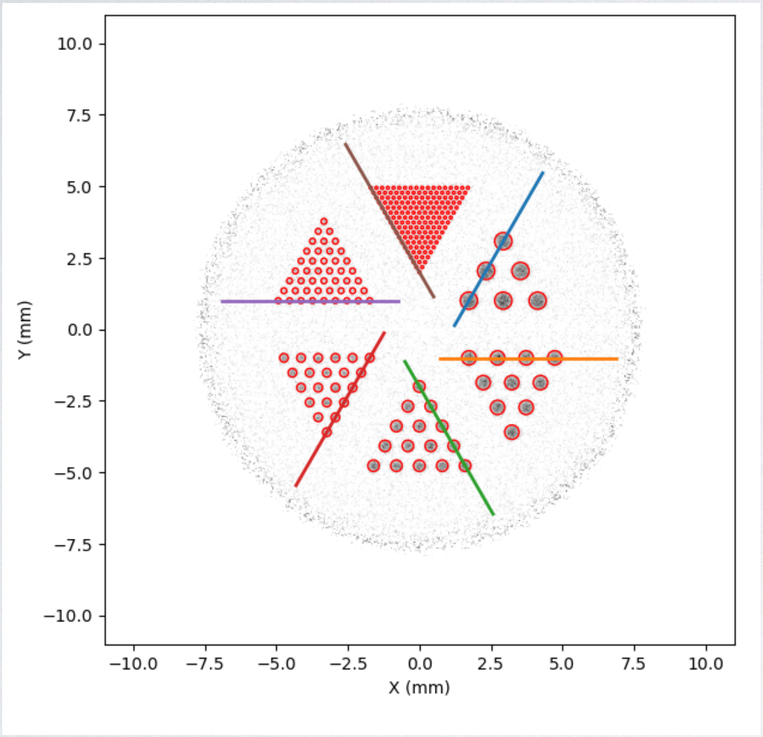
Y (mm)
X (mm)

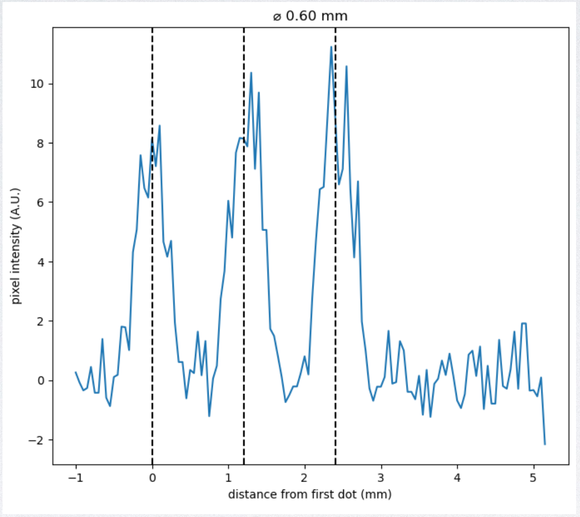
⌀ 0.60 mm
pixel intensity (A.U.)
distance from first dot (mm)

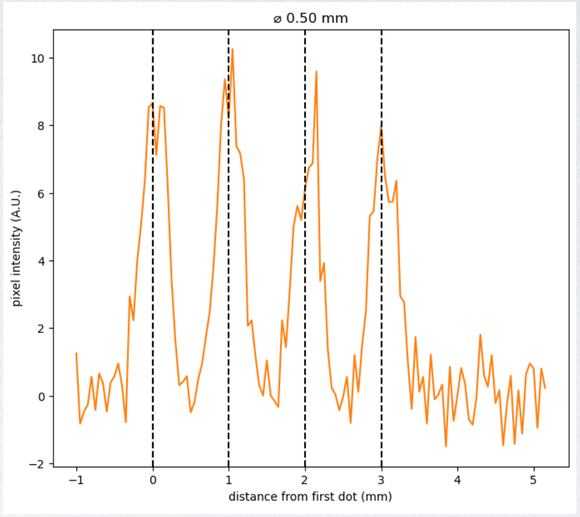
⌀ 0.50 mm
pixel intensity (A.U.)
distance from first dot (mm)

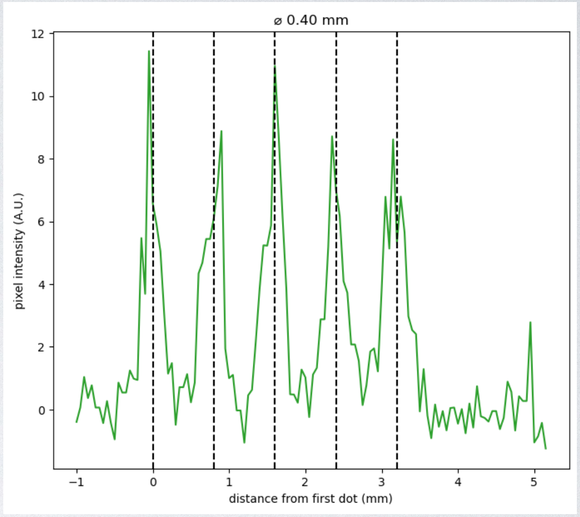
⌀ 0.40 mm
pixel intensity (A.U.)
distance from first dot (mm)

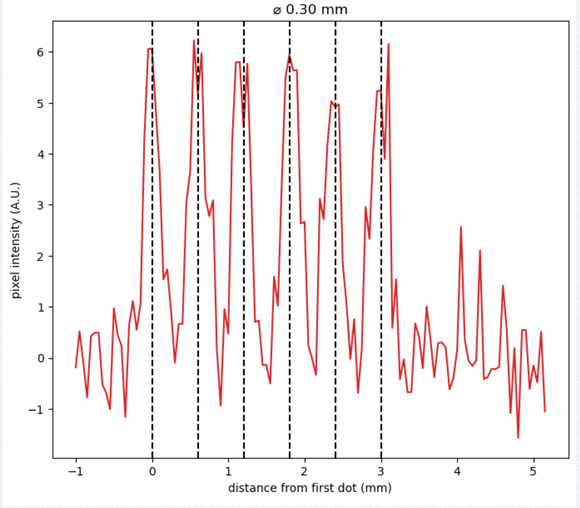
⌀ 0.30 mm
pixel intensity (A.U.)
distance from first dot (mm)

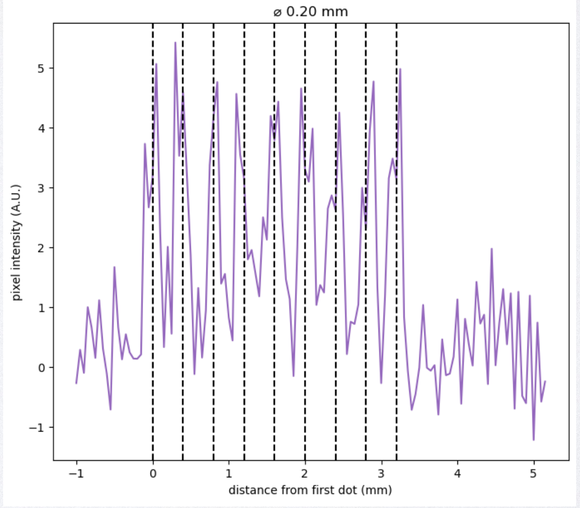
⌀ 0.20 mm
pixel intensity (A.U.)
distance from first dot (mm)

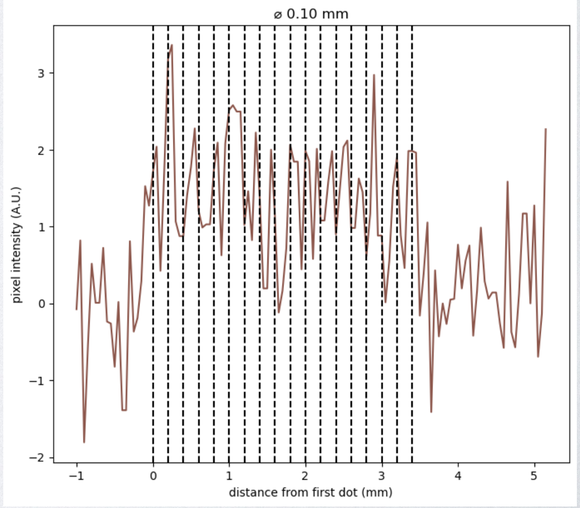
⌀ 0.10 mm
pixel intensity (A.U.)
distance from first dot (mm)

Contrast

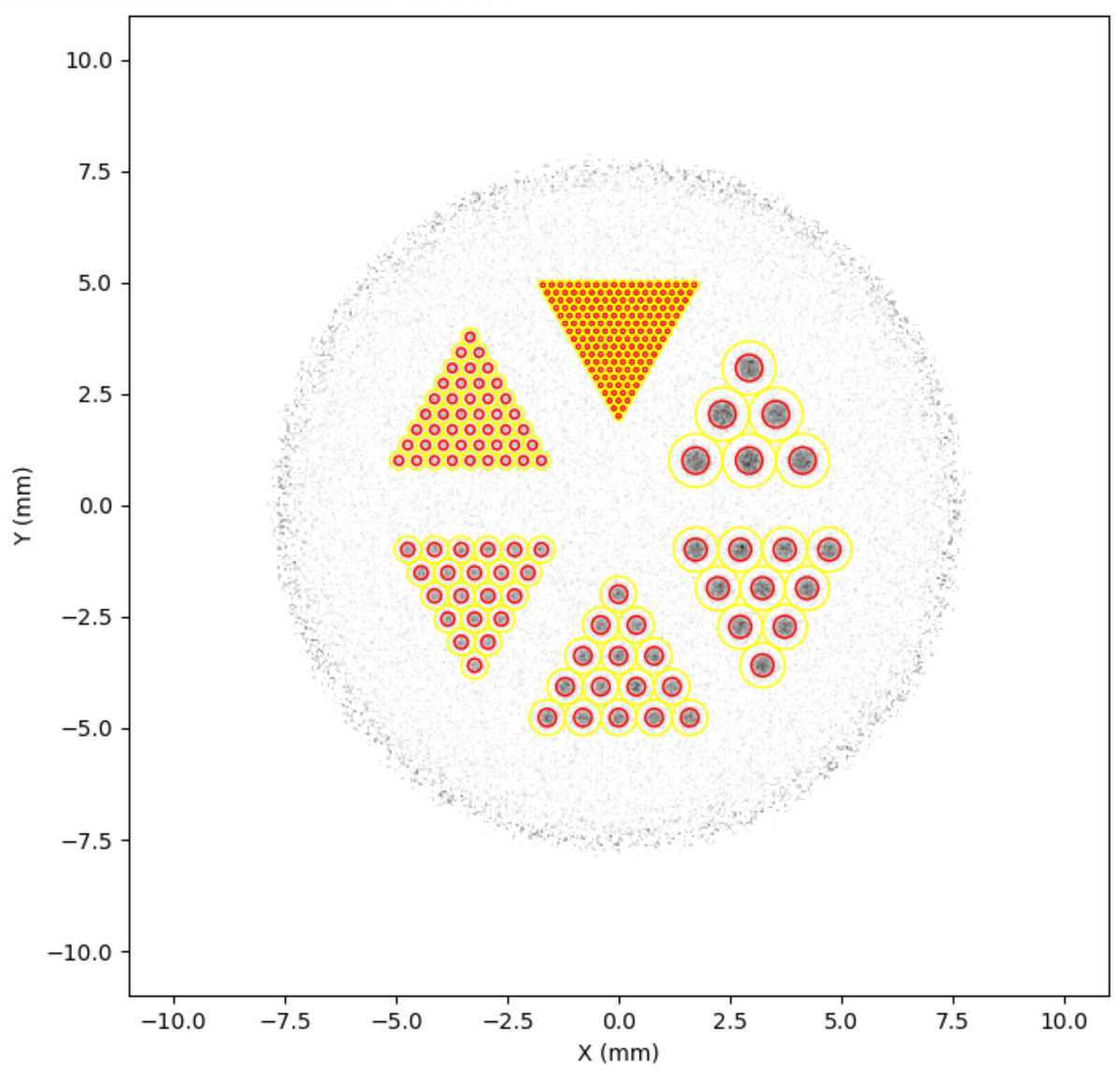

Two ROI defined for each insert :

- **peak value** : ROI centered on insert, with same diameter as the insert (red)
- **valley value** : ROI centered on the insert, with inner diameter same as the insert, and outer diameter twice that of the insert (yellow)

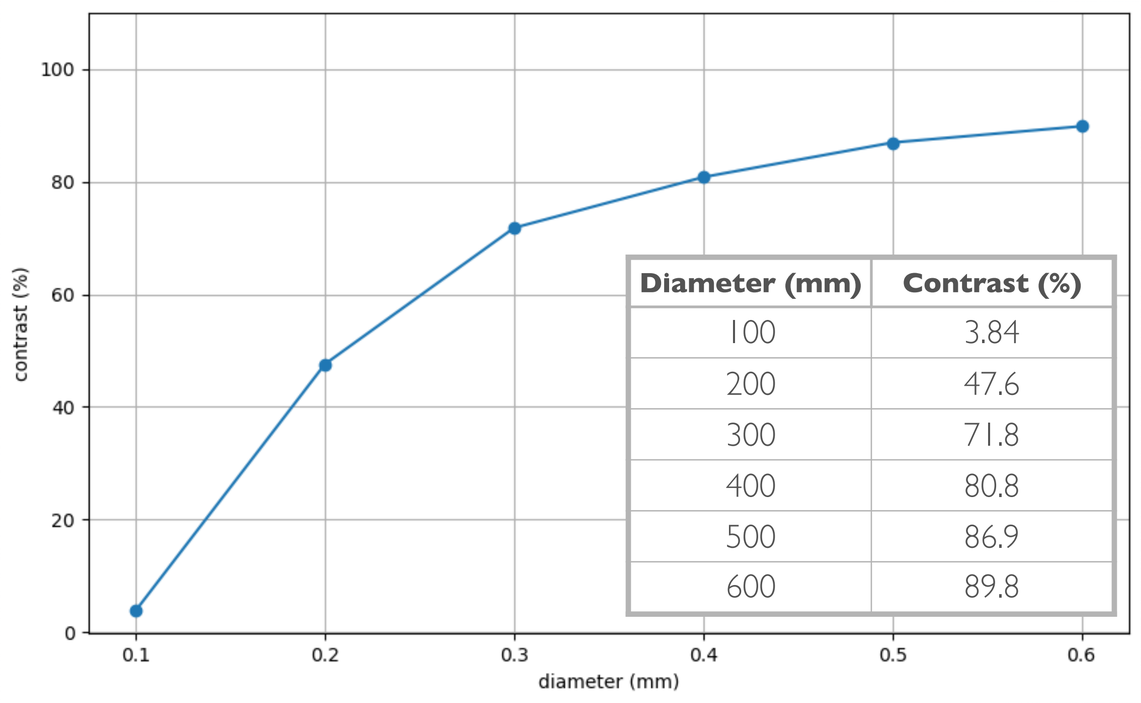

Diameter (mm)	Contrast (%)
100	3.84
200	47.6
300	71.8
400	80.8
500	86.9
600	89.8

Summary

- Application of PALS to biological tissues brings a lot of unknown.
  - Measuring $\tau_{\mathrm{O-Ps}}$ in vivo from bulk tissues require the use of (β+, γ) isotopes to access the positron emission time.
  - New generation of tomographs need enough sensitivity for 3γ events, and good enough coincidence time resolution to be able to measure lifetime differences below 0.1 ns.
  - Need to decorrelate measurement of $\tau_{\mathrm{O-Ps}}$ from the biodistribution.

- TRICERA$\tau_{\mathrm{O-Ps}}$ will solve these issues by proposing a **high activity** $\tau_{\mathrm{O-Ps}}$ measurement **independent of biodistribution**, along with the acquisition of an **anatomical image** from **positron transmission imaging**.

- Positron transmission imaging shows promisses of high resolution imaging of the electronic density of tissues with **structures of order 100 µm**.

Pespectives

- **Sensitivity to various tissue density?**
  - studies underway for evaluating this sensitivity
  - possibility to use metallic contrast agents to improve the capabilities

- Current resolution si limited by the error between the reconstructed position in the tissue layer and the true interaction point, because of high scattering probability of positrons
  ⇒ an **iterative ML-EM reconstruction** is being implemented to better account for this effect

- Simulations have been performed assuming the use of CMOS with a 50µm pixellization, and a 200µm-thick tissue slice, yielding a < 200 µm spatial resolution.
- **Other technologies can be envisioned** for the pixellated layers, and thiner tissue slices can be produced, further improving the expected performance of this new imaging technique
  - If gazeous wire chambers : directionality of incident and outgoing positrons : improved estimation of most probable path

Merci de votre attention